Defence Research and Development Canada | Recherche et développement pour la défense Canada

CAN UNCLASSIFIED

Scattering phase function depolarization parameter model and its application to water droplets sizing using off-axis lidar measurements at multiple angles

Gilles Roy
DRDC – Valcartier Research Centre

Gregoire Tremblay
Aerex Avionic

Xiaoying Cao
Lidar consultant

Applied Optics
Vol. 57, No. 4 / 1 February 2018
p. 969-977

Date of Publication from Ext Publisher: February 2018

Defence Research and Development Canada
External Literature (P)
DRDC-RDDC-2018-P059
May 2018

CAN UNCLASSIFIED

Canada

IMPORTANT INFORMATIVE STATEMENTS

This document was reviewed for Controlled Goods by Defence Research and Development Canada (DRDC) using the Schedule to the *Defence Production Act*.

Scattering phase function depolarization parameter model and its application to water droplets sizing using off-axis lidar measurements at multiple angles

GILLES ROY[1*], GREGOIRE TREMBLAY[2] AND XIAOYING CAO[3]

[1]*Defence Research Development Canada- Valcartier, 2459 de la Bravoure., Québec, QC, Canada, G3X 1X5*
[2]*Aerex Avionic, Canada*
[3]*Lidar consultant, Nepean, ON, Canada*
**Corresponding author: gilles.roy@drdc-rddc.gc.ca*

Received XX Month XXXX; revised XX Month, XXXX; accepted XX Month XXXX; posted XX Month XXXX (Doc. ID XXXXX); published XX Month XXXX

The backscattering lidar depolarization parameter D of water droplets contains information on their size that can be directly modelled as a function of the forward scattering diffraction peak. Using a polarimetric Monte Carlo simulator, water clouds having different extinctions and droplet size distributions are analyzed to estimate their depolarization parameter at various backscattering off-axis angles. It is shown that depolarization parameter of the polarimetric phase function can be found using off-axis lidar measurements at multiple angles, and that it could be used to estimate the water cloud droplets size.

OCIS codes:*(010.1615) Clouds; (010.1350) Backscattering; (010.3640) Lidar; (290.4210) Multiple scattering; (290.5855) Scattering, polarization.*

http://dx.doi.org/10.1364/AO.99.09999

1.0 Introduction and concept

The retrieval of physical properties of atmospheric particles is the common base of all atmospheric lidar work. Using multiple wavelengths and Raman lidars, remarkable results have been obtained on tropospheric particles smaller than the probing wavelengths. Typically, the extinction coefficient, the lidar ratio, and the particles effective radius are derived from these measurements. See [1] for an excellent review of the technique used and results obtained. Water cloud droplets are significantly larger than the probing wavelength and the technique described in Ref.1 cannot be used because the scattering efficiency does not have a dependency over the wavelength. However, water cloud droplets size determination with lidar has been a subject of studies for many years. The proposed technique measures light multiple scattering at multiple field-of-views (MFOV). Physically, the intensity of the forward scattered signal (diffraction peak) as a function of the scattering angle is a function of the ratio of the incident light wavelength over the droplets size. See [2] for an excellent review of the theory and technique used. It remains that the multiple scattering lidar signals are highly convoluted and the extraction of extinction and size is demanding, [3]. Fig. 1 shows how the light is scattered (phase function in red) as a function of the scattering angle for a water cloud made of water droplets with an effective radius of 3.32 µm. It also shows (in blue) the depolarization parameter [4, 5]. This quantity defines how scattering by the droplets affects a polarized laser. The depolarization parameter is the ratio of the secondary polarization phase function over the global phase function at a given angle. This quantity defines how scattering by the droplets affects a polarized laser. Details are provided in section 2 - Depolarization Parameter Model.A MFOV measurement is, to some extent, an indirect measurement of the phase function forward scattering peak because what is being measured is backscattering from multiple forward scattering events toward the detector as illustrated in Fig. 2.

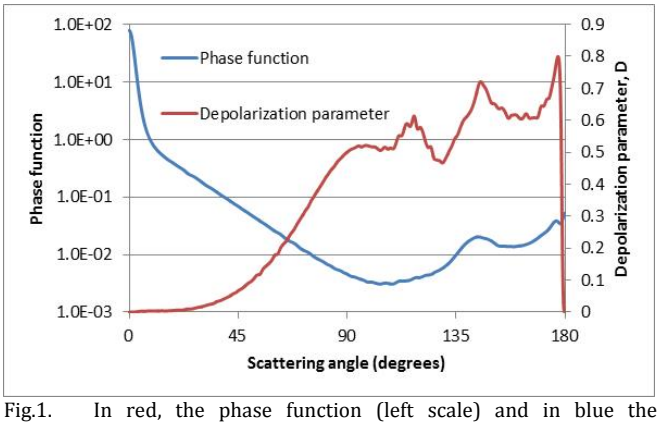

Fig.1. In red, the phase function (left scale) and in blue the depolarization parameter (right scale) as a function of the scattering angle for water droplets having a gamma distribution with a = 3 and b = 1.5 (for and effective radius of 3.32 µm) and an incident wavelength of 532 nm. The phase function exhibits a strong forward scattering peak attributed to diffraction near 0^{o}. The backscattering shows a quasi-constant value with a small increase at 180^{0}. The depolarization parameter, D, is practically equal to zero for scattering angles up to 30^{0}, reaches a very high value near 180^{o} and goes down to 0 at exactly 180^{0}.

Another technique, developed by the University of Pennsylvania [6-8], is to measure multistatic depolarization ratio of the scattered light at angles ranging from 120^{0} to 175^{0}. The multistatic measurements are done with calibrated CCD cameras. The technique works well for low

concentration clouds and has been demonstrated for particles of 1 μm and smaller.

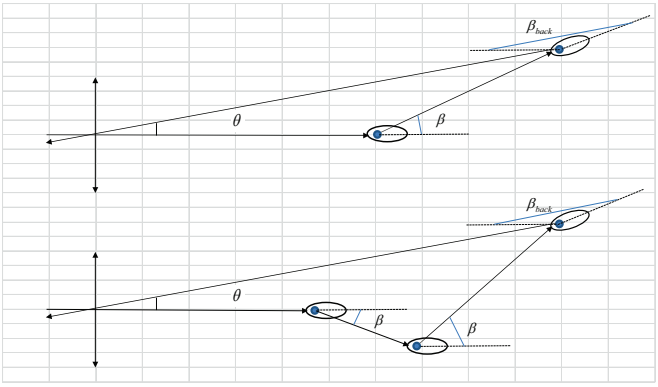

Fig. 2. The signal detected by a lidar at angle θ is the result of backscattering at an angle β_{back} after a double (top), or higher order (bottom), scattering process at various angles β. For small values of the scattering angle β, and large values of β_{back} , the polarimetric phase function displays a strong dependency over the scattering diffraction angle β_b.

In this paper, we propose a method based on the direct measurement of polarized backscattered light at different angles near the 180^0 backscattering direction. A related method is presented in [6, 7] but our concept uses observations at angles that are much closer to 180^0. Doing so, large water droplets can be discriminated as will be demonstrated. Using Mie theory, we will first demonstrate in section 2.0, that the depolarization parameter close to 180^0 is strongly related to the forward scattering diffraction peak and it can be modelled as such. In section 3, the D parameter measurement concept is described, and Monte Carlo (MC) simulations of water clouds having different extinctions and droplet effective radii are performed. In section 4 we compare the D parameter obtained from the MC and the Mie theory and a simple algorithm to derive the droplets size from the D parameter measurement is presented. In section 5, we discuss the D parameter model, the droplets size retrieval technique and experimental feasibility of a measurement system.

2.0 Depolarization Parameter Model

Flynn et al. [4] and Gimmestad [5] have harmonized lidar depolarization theory with radiative transfer theory, particle scattering theory, and standard polarization measurement techniques. They suggested the use of the depolarization parameter (*D*) ranging from 0 to 1 to measure 'the propensity of the scattering medium to depolarize the incident polarization' [5]. They argue there is no reason not to analyze lidar depolarization as any other polarization measurements, i.e., with Stokes vectors and Mueller matrices. Flynn et al. [4] pointed out that symmetry arguments allow substantial cancellation of matrix elements for single scattering on particles having a plane of symmetry or random orientation along the line of sight. D being the only free parameter of the scattering matrix it can be derived from lidar depolarization measurements. The general form of the Mueller matrix that describes a partially depolarizing backward scattering process is

$$M_{atm} = \begin{pmatrix} 1 & 0 & 0 & 0 \\ 0 & 1-D & 0 & 0 \\ 0 & 0 & D-1 & 0 \\ 0 & 0 & 0 & 2D-1 \end{pmatrix}$$

This is interesting because the *D* parameter harmonizes the linear and circular polarization. For linearly and circularly polarized lidar the D parameter is defined as

$$D = \frac{2\delta_{lin}}{1+\delta_{lin}} = \frac{\delta_{cir}}{1+\delta_{cir}} \qquad [1]$$

where δ_{lin} and δ_{cir} are the depolarization ratio defined as the ratio of the perpendicular polarization over the parallel polarization signal. When applied to the polarized phase function, we have

$$D = \frac{p_{\perp}}{p_{//} + p_{\perp}} \qquad [2]$$

where $p_{//}$ and $p_{\perp}$ are the parallel and perpendicular phase function for circular polarization. The use of circular polarization versus the use of linear polarization is discussed in section 3.

Using the Mie theory, we have calculated the phase function and the depolarization parameter as a function of the scattering angle for 6 water cloud profiles represented by the gamma distributions defined in Table 1.
Cumulus clouds of type 1 and 2 are represented using gamma distributions, with parameters (a, b) respectively equal to (7, 1.5) and (4, 0.5). The other distributions parameters have been set to generate water clouds over a broad range of effective radius. The range of droplet size goes from effective radius of 2 μm to 14 μm. The effective radius is defined as $< r^3 > / < r^2 >$. Although these six distributions will be used in Appendix A, our discussion will be centered on the 3.32 μm, 5.99 μm, and 11.92 μm effective radius distributions for clarity.

Table 1 Gamma distribution parameters *a*, *b* and the calculated effective radius, r_e for 6 water cloud profiles.

a	5	4	2	7	3	1
b	0.5	0.5	0.5	1.5	1.5	1.5
$r_e(\mu m)$	13.93	11.92	7.84	5.99	3.32	2.3

Figures 3 and 4 show the Mie theory calculation results. In Fig. 3 we show the forward scattering phase function from 0^0 to 5^0 for droplets with effective radius of 3.32 μm, 5.99 μm and 11.92 μm . In Fig. 4 we show the *D* parameters at backscattering angle ranging from 175^0 to 180^0 for the same distributions.
Simple comparison of Fig. 3 and Fig. 4 suggest a strong relationship between the depolarization parameter *D* and the phase function forward scattering characteristic diffraction angle β_d .

Fig. 5 shows the different variables required to establish a relationship between *D* and β_d . Annex A provides details regarding the parameterization of the depolarization parameter *D* as a function of the phase function forward scattering peak angle β_d . The parameterization is developed for scattering angles ranging from 160^0 to 180^0.

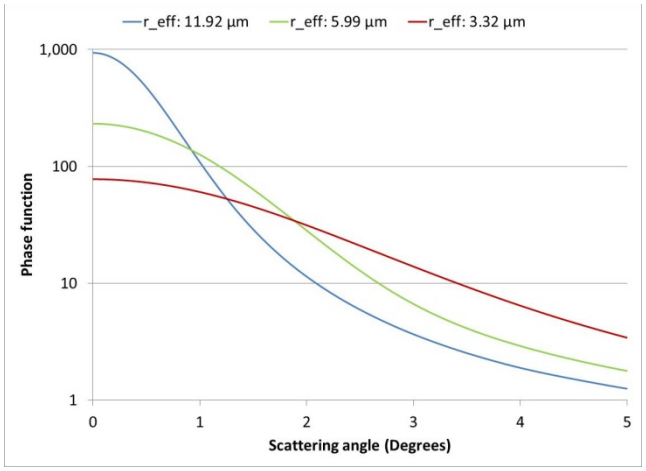

Fig. 3. Droplet size dependence of the phase function forward scattering peak as a function of scattering angle. Incident wavelength is 532 nm. See Table 1 for details of the droplets size distribution.

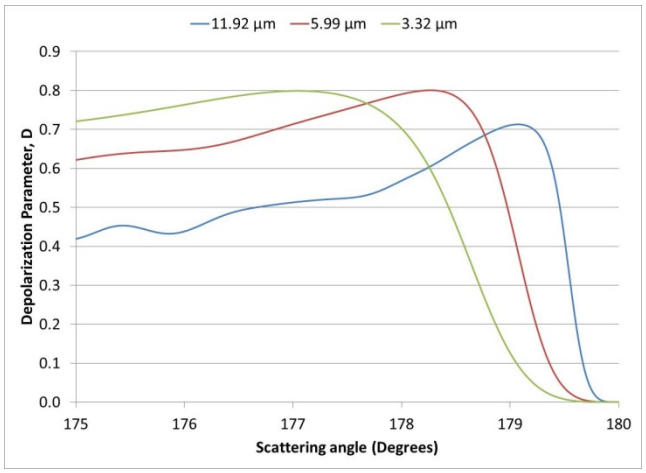

Fig. 4. Depolarization parameter as a function of scattering angle close to backscattering angle. Incident wavelength is 532 nm. See Table 1 for details of the droplets size distribution. Positions of the maximum of the depolarization parameters exhibit a clear droplets size dependency.

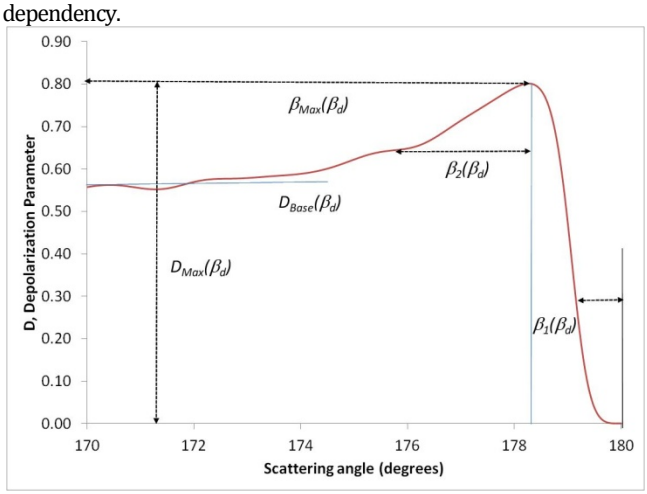

Fig. 5. Parameterization of the D parameter as a function of the forward scattering phase function diffraction peak.

As in [9] the forward scattering phase function is modelled as a Gaussians with width equal to

$$\beta_d = 0.585(\lambda / 2r_e), \qquad [3]$$

where, r_e is the effective radius, λ is the wavelength, and β_d is the width of the diffraction peak.

For scattering angle greater than $\beta \geq \beta_{Max}$, a super-Gaussian provides an excellent fit of the D parameter:

$$D(\beta, \beta_d) = D_{Max}(\beta_d)[1 - \exp{-((\pi - \beta)/(w_1\beta_1)^4}], \qquad [4]$$

For scattering angle smaller than $\beta < \beta_{Max}$, the D parameter can be represented by

$$D(\beta, \beta_d) = D_{Max}[\exp{-(-(\beta_{\max} - \beta)/(w_2\beta_2))}] + D_{base}, \qquad [5]$$

The various parameters used to represent the D parameter in Eq. 4 and Eq. 5 for scattering angle ranging from 160^0 to 180^0 are

a) the position of the maximum $\beta_{Max}(\beta_d)$, that varies linearly with β_d, $\beta_{Max}(\beta_d) = -0.9233\beta_d + 179.67^o$;

b) the offset parameter $D_{base}(\beta_d)$, that varies with β_d and can be represented as

$$D_{base}(\beta_d) = 0.1568\ln(\beta_d) + 0.4441;$$

c) the maximum value of depolarization parameter, $D_{Max}(\beta_d)$, that does not vary much with β_d and is practically constant with mean value $D_{Max}(\beta_d) = 0.754$;

d) the super-Gaussian characteristic angle is provided by

$\beta_1 = 0.6592\beta_d$;

e) the exponential decay characteristic angle is provided by

$\beta_2 = 1.2787\beta_d$;

f) and two fit parameters

w1 = 0.93 and w2 = 1.37.

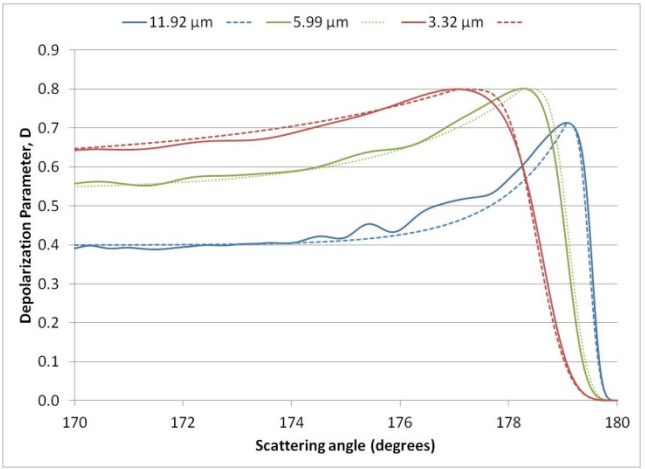

Fig. 6 Comparison between the *D* parameters obtained using the Mie theory (solid curves) and the parameterized D (dashed curves) obtained using the model. The incident wavelength is 532 nm. The

droplet size distribution follows a gamma distribution defined in Table 1.

In short, $D(\beta, r_e)$ starts from a value of zero at 180^0 and increases quickly following a super-Gaussian. The width of the super-Gaussian is linearly related to the width of the forward scattering peak β_d. Passed the maximum value, in the direction of decreasing angles, $D(\beta, \beta_d)$ decreases exponentially at a rate linearly related to β_d. Fig. 6 provides a comparison between the D parameters obtained using the Mie theory and the parameterized D obtained with the model. The incident wavelength is 532 nm. The droplet size distribution follows a gamma distribution defined in Table 1. The fits are plainly satisfactory.

3.0 *D* parameter measurement concept and Monte Carlo simulations

The fact that direct measurement of the depolarization parameter leads to information on droplets size is the concept backbone. To get this information, it is necessary to perform off-axis lidar measurements as displayed in Fig. 7a. The relationship between the nearly backscattering angle β and the probing angle β_i is $\beta_i = \pi - \beta$ The characteristics of the lidar are

- a single circularly polarized laser beam,
- multiple receivers having polarimetric detection capabilities to capture backscattering, ;
- and probing angles $\beta_i = x_i / z$ defined by the ratios of the off-axis distances x_i over the probing rage z..

The receiver polarimetric detection is provided by a quarter wave-plate set at 45^0 to convert the circular polarization into the two linear polarizations separated by a polarizing cube beam splitter and imaged on two independent detectors (ideally two Gated ICCD cameras). The measurement of a specific position of the laser beam is performed at various angles with a series of telescopes distributed along the horizontal axis. For circular polarization, D is independent of the scattering azimuthal angle ϕ while linear polarization shows a strong azimuthal dependency in $\cos^4\phi$, [10-14]. Using circular polarization, we make sure that the measurements are independent of the azimuthal angle.

The use of Monte Carlo (MC) to demonstrate scattering effects on depolarization by water clouds in presence of multiple scattering is a powerful tool that has led to Hu relationship [15] presently used for the analysis of the space lidar Caliop. In here, we use the Undique [16] imaging MC simulator. It is a multithread software based on the Bohren and Huffman Mie scattering computation routine. The simulator is made to reproduce the characteristics of an actual Flash Lidar system. It consists of an emitter/receiver system, a target and a propagation range including aerosols of various properties. The particularity of the Undique MC is its capability to image the scattered light on a detector array. In here, the imaging system is made of 256 x 256 pixels with a 2 mrad x 2 mrad FOV. The simulated system characteristics are provided below.

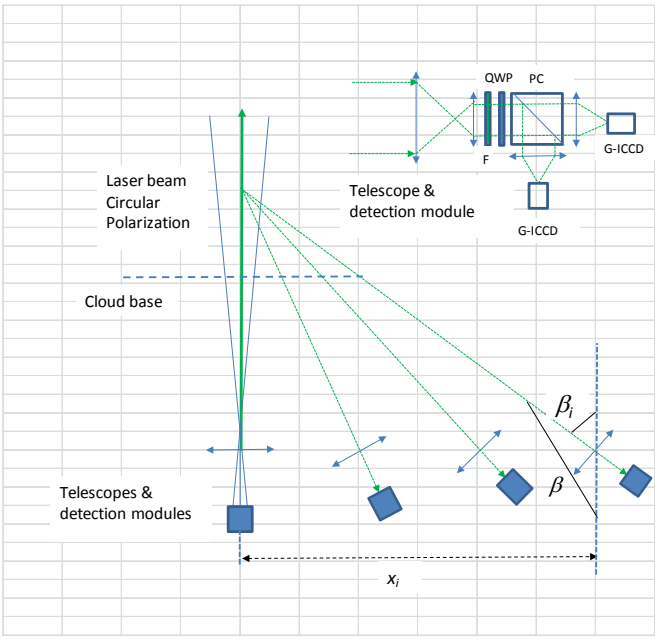

Fig. 7a. Lidar off-axis measurement of backscattered light. The laser beam is pointed vertically, and a series of receivers with polarimetric detection capability point toward the same laser illuminated volume.

Laser :

- beam divergence: 0.3 mrad
- wavelength: 532 nm
- Polarization: Circular

Collecting optic:

- 20 cm in diameter
- focal length: 0.76 m
- Waveplate: $\lambda/4$
- Polarizer: horizontal & vertical for principal and secondary polarization detection

Water clouds characteristics:

- Cloud base: 500 m
- Extinctions: one cloud with extinction growing linearly by 0.005 m^{-1} times the penetration depth, and a cloud with constant extinction of 0.03 m^{-1}
- Droplet size distributions: Gamma distributions with a = 4, b = 0.5; a = 7, b = 1.5, and a = 3, b = 1.5 for effective radius of 11.92 µm, 5.99 µm and 3.32 µm respectively.

The 15 off-axis distances are set to provide backscattering angle measurements ranging from 0 mrad to 30 mrad at probing ranges of 500 m. The probing angles are selected to sample the transition of the Depolarization parameter that goes from 0, at 180^0, to various phase function related values. We made sure the sampling angles would enable us to discriminate 3 different water clouds.

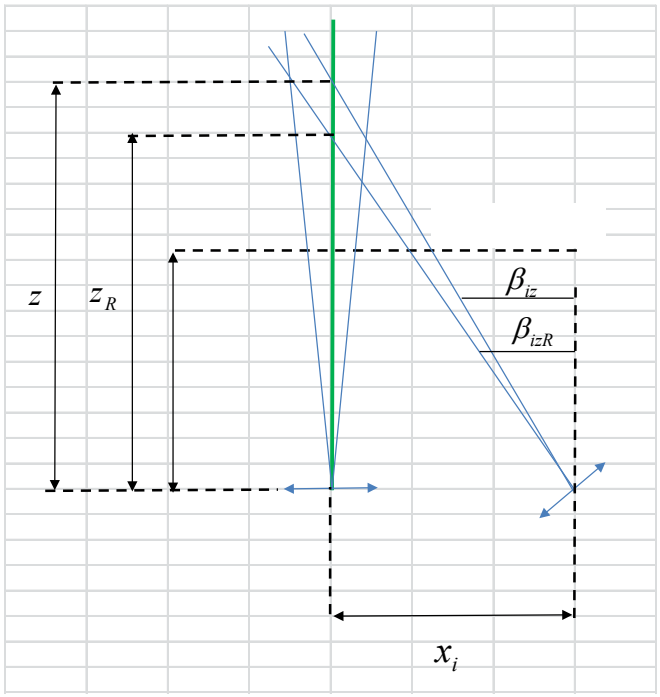

Fig. 7b. Lidar off-axis measurement of backscattered light. Definition of variables.

As shown on Fig. 7b, probing is done at a range z_R with off-axis angles β_{iz} ranging from 0 mrad to 30 mrad by steps of 2 mrad. In the following, the indices *'i'* goes from 0 to 15. The distance x_i for a probing distance z_R is $x_i = z_R \beta_{izR}$. The images are centered on the G-ICCD at the distance z_R for all probing angles.Images can be used below and above the distance z_R as long as the laser beam foot print is completely inside the camera FOV. Atdistance z_i the off-axis angle is $\beta_{iz} = x_i / z$, and the position of the center of the laser beam (B_{center}) such as seen by the G-ICCD camera is $B_{center}(Pixel)_{iz} = 256(\beta_{izR} - \beta_{iz})/FOV$, where FOV= 0.002 rad.

Fig. 8 and Fig. 9 are obtained with the Undique MC simulator. We show backscattered signal for the principal and secondary polarization as seen by co-axial (0 mrad) and off-axis detection at 10 mrad, 20 mrad, and 30 mrad. Each image is 2 mrad x 2 mrad and the laser beam divergence is 0.3 mrad. The cloud is made of water droplets of effective radius of 5.95 µm (see Table 1 for details). In Fig. 8 the cloud base is 500 m from the receiver, the images are obtained at cloud depth of 4 m for an optical depth of 0.04. Following the prevailing convention, the optical depth (OD) is defined as OD = -ln(transmission). For small optical depth penetration, multiple scattering did not build up and the backscattered light comes mainly from direct backscattering from the laser beam. The laser beam backscattered light is surrounded by some very sparse multiple scattered light. For backscattering at 180^0 (0 mrad measurements) the secondary polarization shows values close to zero.

In Fig. 9, the cloud base is still 500 m from the receiver and the extinction is 0.03 m^{-1}. The images are obtained at cloud penetration depth of 34 m for an optical depth of 1.02. The laser beam backscattered light is surrounded by multiple scattering. In the lower right image, (s polarization and 30mrad off-axis detection), we show the different FOVs used for the analysis: 0.3 mrad, 1 mrad, and 2 mrad.

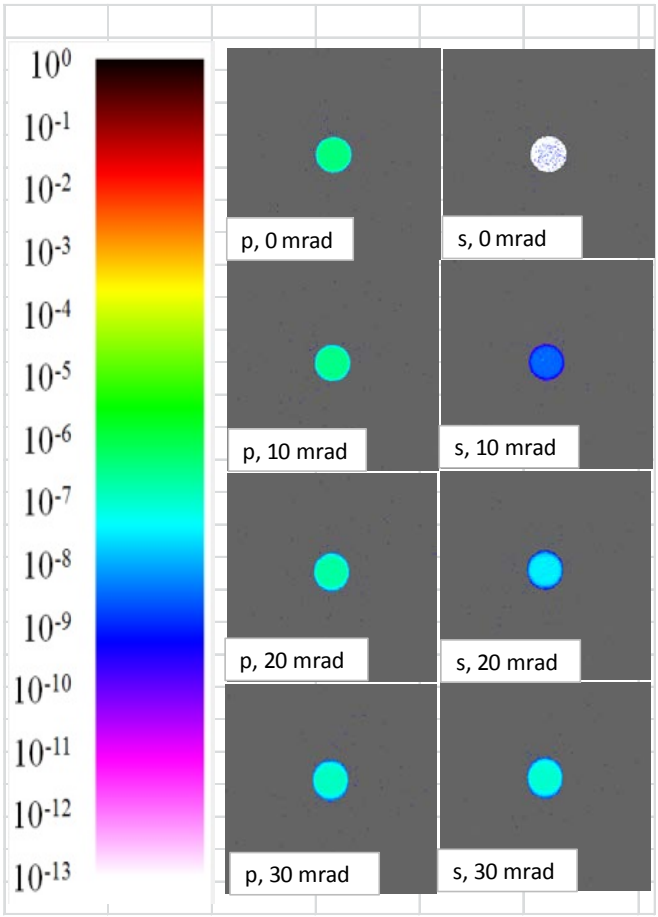

Fig.8. Images obtained with Undique MC simulator. We show the backscattered light for the principal and secondary polarization as seen by co-axial (0 mrad) and off-axis detection at 10 mrad, 20 mrad and 30 mrad. Each image is 2 mrad x 2 mrad. The cloud is made of water droplets of effective radius of 5.95 µm (see Table 1 for details). The cloud base is 500 m from the receiver, the images are obtained at cloud depth of 4 m for an optical depth of 0.04. The laser beam backscattered light is surrounded by some very sparse multiple scattering.

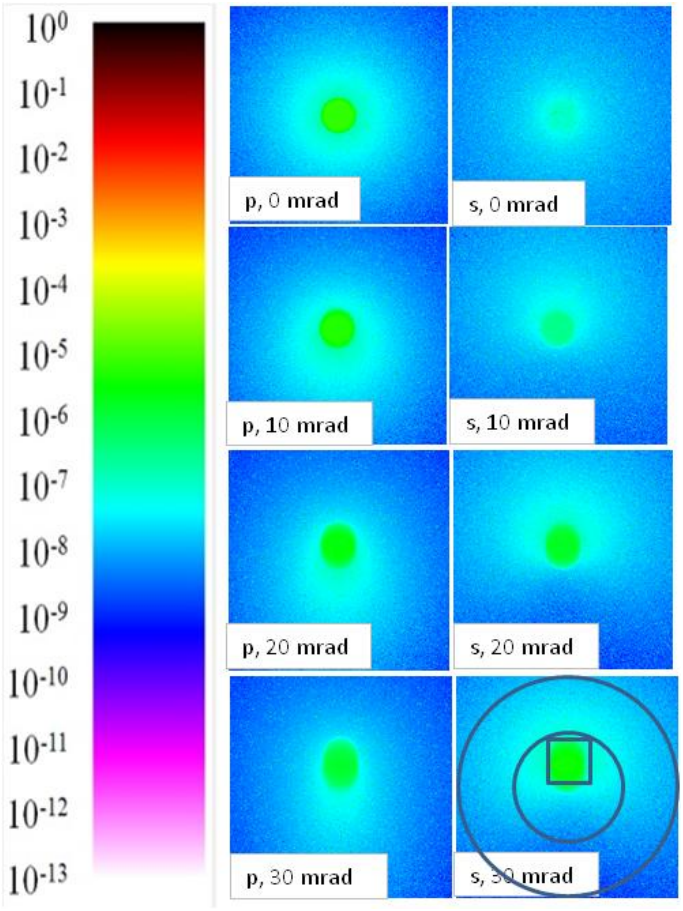

Fig.9. Images obtained with Undique MC simulator. We show backscattered light for the principal and secondary polarization as seen by co-axial (0 mrad) and off-axis detection at 10 mrad, 20 mrad and 30 mrad. Each image is 2 mrad x 2 mrad. The cloud is made of water droplets of effective radius of 5.95 μm (see Table 1 for details). The cloud base is 500 m from the receiver, the extinction is 0.03 m^{-1} and the images are obtained at cloud penetration depth of 34 m for an optical depth of 1.02. The laser beam backscattered light is surrounded by multiple scattering. In the lower right image, (s, 30 mrad), we show the 0.3 mrad, 1 mrad, and 2 mrad FOVs used for the analysis.

4.0 Analysis: comparison of MC *and* Mie theory *D* parameter results

MC analysis consists in calculating D for three of the clouds listed in Table 1. Most of the analyses are performed for a FOV of 0.3 mrad. Given that the measurements are done at different off-axis angles, the position of the laser beam such as seen by the detection system will change with the off-axis angle, and with the laser beam penetration depth. The 0.3 mrad analyses are always performed centered on the laser beam centroid. The 1 mrad and 2 mrad FOVs analysis have been limited to an OD of 1. Fig. 9 (s, 30 mrad) shows the 0.3 mrad FOV centered on the laser beam and the fix 1 mrad and 2 mrad FOVs.

Fig. 10a to 10c compare the D parameter, as a function of the off-axis angle, for three droplet sizes as calculated by the MC, with by using the model based on polarimetric phase function described in section 2 and appendix A. For backscattering angle greater than β_{Max} the depolarization parameter is set equal to

$$D(\beta_{iz}, r_e) = 0.75[1 - \exp-(\beta_{iz})/(0.85\beta_d))^4]. \qquad [6]$$

For droplets size equal to 3.32 μm and 5.99 μm, *D* can be represented using only equation [4]. For the larger droplet size (11.92 μm) equation [5] is also used to represent the exponential decay of *D* for off-axis angle beyond D_{Max} location.

In Fig. 10a and Fig. 10b, the *D* parameter is calculated for the 0.3 mrad FOV; in 10a, the optical depths are very small (0.04 and 0.21), while in 10b, optical depths are equal to 1.02, 1.47 and 1.7. The MC simulation results are identified with symbols, while the model results are represented with solid curves.

In Fig. 10c, the effect of FOV is studied and the *D* parameter is calculated for FOV of 0.3 mrad, 1 mrad, and 2 mrad for an optical depth equal to 1.02. For the small 0.3 mrad FOV, the *D* parameters (represented with solid curves) match reasonably well the MC off-axis lidar simulation of Fig 10 a, b; for the larger FOVs, depolarization caused by multiple scattering appears to be dominant at small off-axis angles.

The MC results agree reasonably well with the *D* parameter results considering the model does not take into account the laser beam divergence and the collection optic FOV.

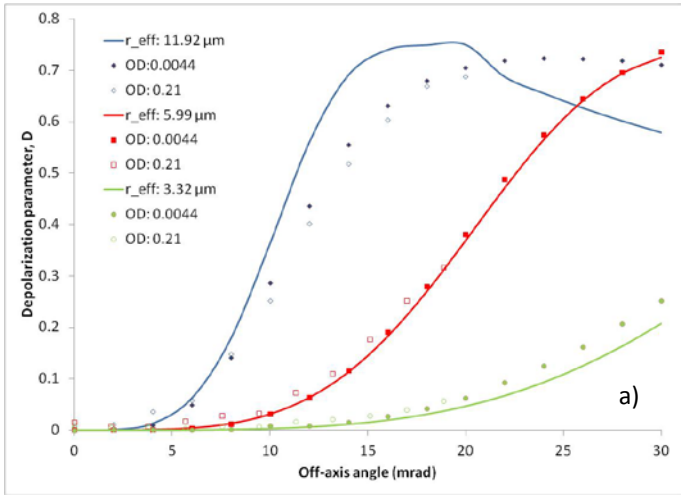

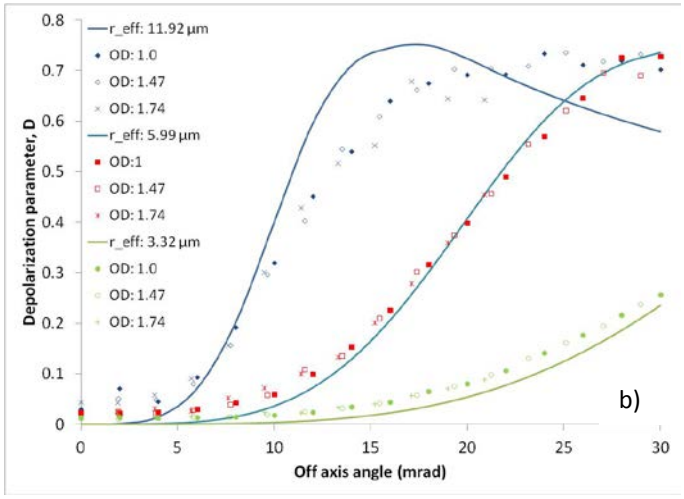

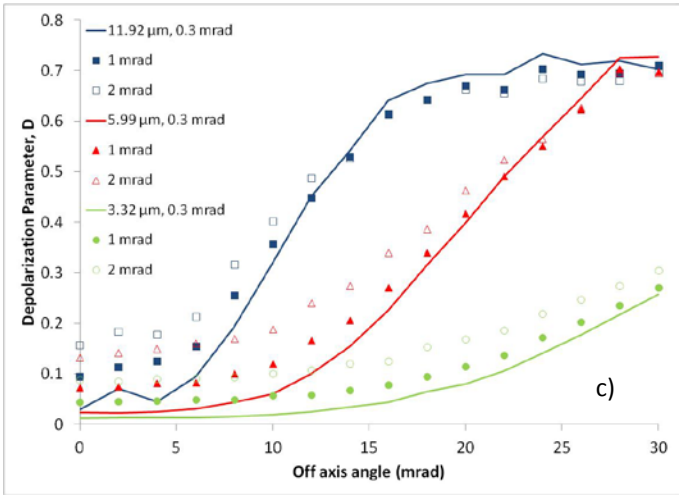

Fig. 10 Comparison of MC depolarization parameters with the Mie calculated D parameters as a function of the off-axis tilt angle. In 10a and 10b, the D parameters are calculated for the 0.3 mrad FOV; in 10a, the optical depths are very small (0.0044 and 0.21), while in 10b, OD equal to 1, 1.47 and 1.7. In 10c, the D parameters are calculated for FOV of 0.3 mrad, 1 mrad and 2 mrad; the optical depth is equal to 1.02.

4.1 Droplet size retrieval

Results obtained for the 0.3 mrad FOV suggest it is possible to retrieve the droplets size. Rearranging Eq. [6] and using Eq. [3] to replace β_d we get

$$r_e = 0.29\lambda\left[-\ln(1 - D(\beta_{iz}, r_e)/0.75)\right]^{1/4} / \beta_{iz}\,. \qquad [7]$$

Using Eq. [7], a comparison of the retrieved droplets size as a function of the off-axis angles is shown in Fig. 11 for the 0.3 mrad FOV results (solid curves) and for different ODs (symbols).
For the larger ODs, multiple scattering effects are noticeable for off-axis angle up to 10 mrad. The use of Eq. [7] for droplets size retrieval is very basic (it uses a single off-axis measurement to estimate the size) and is sufficient to demonstrate the concept of droplets size retrieval. However, it has important limitations; for example, a measurement performed at angles greater than 20 mrad will not allow distinction between the 5.99 µm and 11.92 µm droplet. An algorithm using multiple off-axis measurement would allow unambiguous droplet size retrieval.

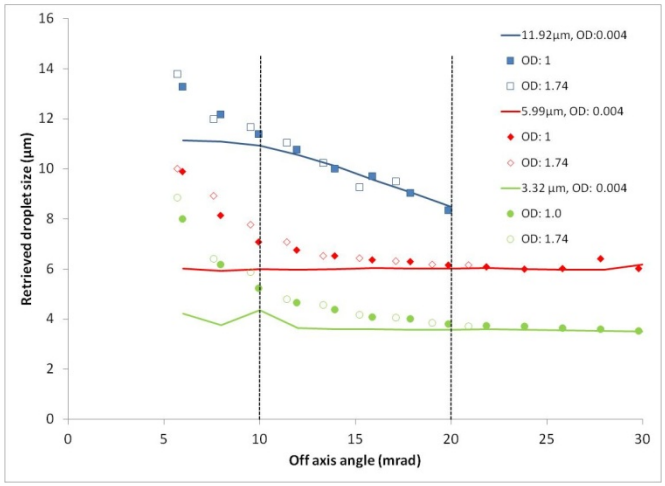

Fig 11. Comparison of the water droplets retrieved size as a function of the off-axis angle. The 0.3 mrad FOV results have been used. For the larger ODs, multiple scattering effects are noticeable for off-axis angle up to 10 mrad.

5.0 Discussion and conclusion

We have demonstrated the proof of concept for the determination of water cloud droplet size measurement. To achieve that goal we first modelled the *D* parameter from 160^0 to 180^0 as a function of the phase function forward scattering angle β_d. Since β_d is proportional to the ratio $\lambda / 2r_e$, a measure of *D* will lead to information on the water droplet effective radius.

Then we used an imaging MC to simulate *D* parameter lidar measurements at off-axis angle ranging from 0 mrad to 30 mrad on water cloud of different extinctions and water droplet sizes. Third, we compared the *D* parameter obtained from these simulations with the *D* parameter calculated using the polarimetric phase function. This comparison confirms that off-axis lidar measurements are indeed a measurement of the *D* parameter. Finally, a simple equation has been derived to demonstrate it is possible to retrieve the water droplet size using the *D* parameter measured at a specific angle.

The measurements of the *D* parameter at different off-axis angles appear not to be much sensitive to multiple scattering effects. This is mainly due to the fact that forward scattering does not depolarize significantly the incident light. The laser beam, as well the forward scattered light, reach the position of interest while maintaining polarization state until the backscattering induces depolarization at off-axis angles. The level of depolarization is maintained on the way to the receiver even if the light undergoes multiple forward scattering at relatively small angles.

There is much to do to validate the concept and push further its application. Although, MC calculations are known to reflect the real word (see the work of Hu & al [15]), experimental validations need to be performed. Adaptation of the experimental set up of Akamoto and Sato [17] could be considered for an experimental validation.

The droplets size retrieval algorithm is very basic and can certainly be improved by curve fitting algorithms and defining the best set of probing angles.

Water droplet clouds may contain ice crystals or snow that will depolarize the incident light at 180^0. These particulates will create an offset at 180^0 but most likely, the propose methodology can be studied/adapted to retrieve water cloud droplet size.

Finally, a multiple axis lidar is presently under construction. It will consist of a polarimetric system and multiple laser beams illuminating (in circular polarization) the cloud sequentially at different angles.

Appendix A

Modelization of the Depolarization Parameter near the backscattering angle

The forward scattering phase function is modelled as a summation of Gaussians [9]

$$p(r,\beta) = \frac{1}{2}\frac{1}{\pi\beta_d}\exp(-\beta^2/{\beta_d}^2) + \frac{A_g}{2}\frac{1}{\pi\beta_g}\exp(-\beta^2/{\beta_g}^2),$$

where

$\beta_d = 0.585(\lambda/2r_e)$, $\beta_g = 0.481$; and $A_g = 0.89$,

where r_e is the effective radius, λ is the wavelength, β_d is the width of the diffraction peak, and β_g is the width of the geometrical optic component (units are in rad).

D has been calculated for 6 gamma distributions described in Table 1.

The five parameters identified in Fig. 5 to model *D* as a function of β_d are shown in Fig. A1 to A5.

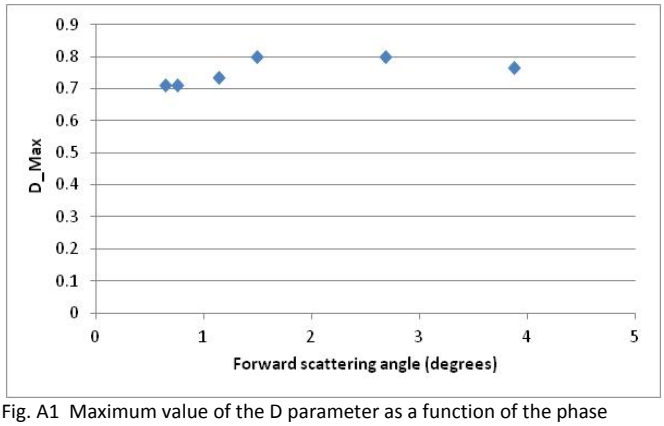

Fig. A1 Maximum value of the D parameter as a function of the phase function forward scattering peak.

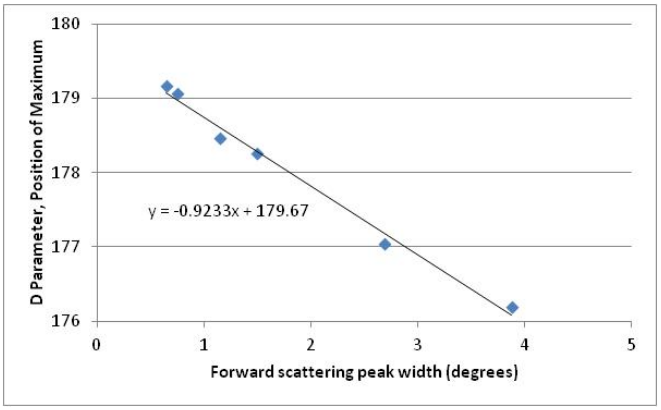

Fig. A2 Position of the maximum value of the D parameter as a function of the phase function forward scattering peak, β_d.

$D_{Max}(\beta_d)$ is practically independent of β_d with a mean value equal to 0.754, see Fig. A1.
However, based on Fig. A2, the position of the maximum varies linearly with β_d

$\beta_{Max}(\beta_d) = -0.9233\beta_d + 179.67^o$;

if we force a value of 180^0 for β_d equal to 0, the position of the maximum value is $\beta_{Max}(\beta_d) = 180^o - \beta_d$.

The depolarization parameter for backscattering angles from 160^0 to 180^0 is related to the forward scattering peak characteristic angle. The mathematical representation is

If, $\beta \geq \beta_{Max}$, $D(\beta, r_e) = D_{Max}(\beta_d)[1 - \exp-((\pi - \beta)/(w_1\beta_1)^4]$,
with, $\beta_1 = 0.6592\beta_d$, see Fig. A3

If, $\beta < \beta_{Max}$,

$D(\beta, \beta_d) = D_{Max}(\beta_d)\cdot\exp(-(\beta_{\max} - \beta)/(w_2\beta_2(\beta_d)) + D_{base}(\beta_d)$,

with, $D_{base}(\beta_d) = 0.1568\ln(\beta_d) + 0.4441$ (see Fig. A5), and $\beta_2 = 1.2787\beta_d$ (see Fig. A4).

The fit parameters w_1 and w_2 are also practically independent of β_d with a mean values equal to 0.93 and 1.37 respectively (see Fig. A6).

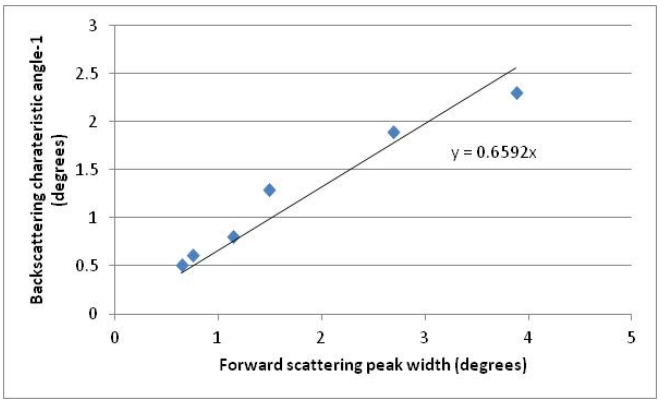

Fig. A3 Super-Gaussian characteristic angle as a function of the phase function forward scattering peak, β_d .

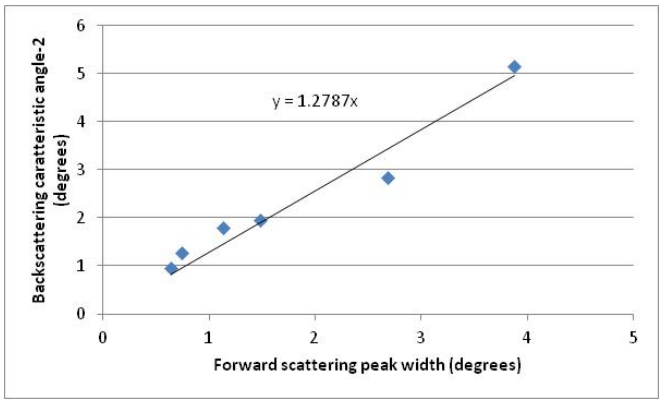

Fig. A4 Exponential decay characteristic angle as a function of the phase function forward scattering peak, β_d .

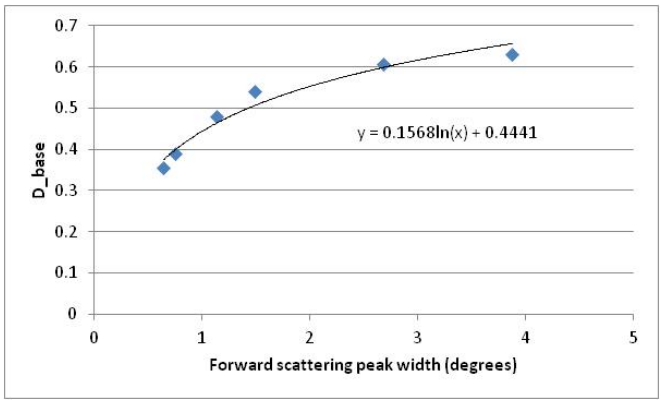

Fig. A5 Asymptotic constant value of the D parameter as a function of the phase function forward scattering peak, β_d .

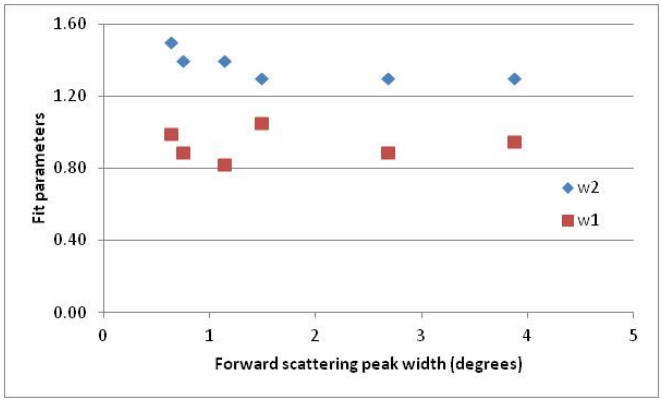

Fig. A6 Correction factors, w_1 and w_2 applied to the super-Gaussian fit and to the exponential fit width as a function of the phase function forward scattering peak, β_d .

In short, $D(\beta, \beta_d)$ starts with a value of zero at 180^0 and increases quickly following a super-Gaussian. The width of the super-Gaussian is linearly related to the width of the forward scattering peak β_d . Past the maximum value, in the direction of decreasing angles, $D(\beta, \beta_d)$ decreases exponentially and the decrease rate is linearly related to β_d .

References

1. A. Ansmann and D. Muller, "Lidar and atmospheric Aerosol", Ch 4 of Lidar: Range resolved optical remote sensing of the atmosphere/Clauss Weitkamp, Spinger, 2005, ISSN 0342-4111; 102

2. Luc R. Bissonnette, "Lidar and multiple scattering", Ch 4 of Lidar: Range resolved optical remote sensing of the atmosphere/Clauss Weitkamp, Spinger, 2005, ISSN 0342-4111;102

3. L. R. Bissonnette, G. Roy and N. Roy, " Multiple-scattering-based lidar retrieval: method and results of cloud probings", Appl. Opt. 44, 5565– 5581 (2005)

4. C. J. Flynn, A. Memdoza, Y. Zheng, and S. Mathur, "Novel polarization-sensitive micropulse lidar measurement techniques," Opt. Express 15, 2785–2790 (2007).

5. G. G. Gimmestad, "Reexamination of depolarization in lidar measurements," Appl. Opt. 47, 3795–3802 (2008).

6. A. M. Brown, "Multiwavelength multistatic optical scattering for aerosol characterization", PhD Thesis, Pennsylvania State University, August 2010

7. Michelle G. Snyder ; Andrea M. Brown and C. Russell Philbrick "Sensitivity of the polarization ratio method to aerosol concentration", *Proc. SPIE* 8037, Laser Radar Technology and Applications XVI, 80370K (June 08, 2011); doi:10.1117/12.884206; http://dx.doi.org/10.1117/12.884206

8. J.H. Park, "Multiple scattering measurements using multistatic lidar', PhD Thesis, Pennsylvania State University, May 2008

9. L. R. Bissonnette, G. Roy, L. Poutier, S. G. Cober, and G. A. Isaac, "Multiple-scattering lidar retrieval method: tests on Monte-Carlo simulations and comparisons with in situ measurements," Appl. Opt. 41, 6307– 6324 (2002)

10 S. R. Pal and A. I., Carswell, Polarization anisotropy in lidar multiple scattering from atmospheric clouds, *Appl. Opt.*, **24**, 3464-3471 (1985).

11. N. Roy, G. Roy, L. R. Bissonnette and J-R. Simard, Measurement of the azimuthal dependence of cross-polarized lidar returns and its relation to optical depth, *Appl. Opt.* **43**, 2777-2785, (2004)

12. V. Griaznov, I. Veselovskii, P. Girolamo, M. Korenskii and D. Summa, Spatial distribution of doubly scattered polarized laser radiation in the focal plane of a lidar receiver, *Appl. Opt.* **46**, 6821-6830, (2007)

13. A. Doroshkevich, The effect of droplet cloudy microstructure on the polarization characteristics of double scattering lidar return, *SPIE* Vol. 10035, 1003550, (2016)

14. G. Roy & N. Roy , Relation between circular and linear depolarization ratios under multiple-scattering conditions Appl. Opt. 47, 6563-6579 (2008).

15 Y. Hu, et al., “Simple relation between lidar multiple scattering and depolarization for water clouds,” Opt. Lett. 31, 1809–1811 (2006).
16 G. Tremblay, G. Roy, High fidelity imaging algorithm for the Undique Monte Carlo simulator. *27rd International Laser Radar Conference,* New York, USA, (2015)
17 H. Okamoto, K, Sato, T. Nishizawa, N. Sugimoto, T. Makino, Y. Jin, A. Shimizu, T. Takano and M. Fujikawa, “Development of a multiple-field-of-view multiple-scattering polarization lidar: comparison with cloud radar”, Opt. Express 25, 30054-30067 (2016)

DOCUMENT CONTROL DATA

*Security markings for the title, authors, abstract and keywords must be entered when the document is sensitive

1. ORIGINATOR (Name and address of the organization preparing the document. A DRDC Centre sponsoring a contractor's report, or tasking agency, is entered in Section 8.)

OSA—The Optical Society
2010 Massachusetts Ave., N.W.
Washington, D.C. 20036-1012 USA

2a. SECURITY MARKING (Overall security marking of the document including special supplemental markings if applicable.)

CAN UNCLASSIFIED

2b. CONTROLLED GOODS

NON-CONTROLLED GOODS
DMC A

3. TITLE (The document title and sub-title as indicated on the title page.)

Scattering phase function depolarization parameter model and its application to water droplets sizing using off-axis lidar measurements at multiple angles

4. AUTHORS (Last name, followed by initials – ranks, titles, etc., not to be used)

Roy, G.; Tremblay, G.; Cao, X.

5. DATE OF PUBLICATION (Month and year of publication of document.)	6a. NO. OF PAGES (Total pages, including Annexes, excluding DCD, covering and verso pages.)	6b. NO. OF REFS (Total references cited.)
February 2018	10	17

7. DOCUMENT CATEGORY (e.g., Scientific Report, Contract Report, Scientific Letter.)

External Literature (P)

8. SPONSORING CENTRE (The name and address of the department project office or laboratory sponsoring the research and development.)

DRDC - Valcartier Research Centre
Defence Research and Development Canada
2459 route de la Bravoure
Quebec (Quebec) G3J 1X5
Canada

9a. PROJECT OR GRANT NO. (If appropriate, the applicable research and development project or grant number under which the document was written. Please specify whether project or grant.)	9b. CONTRACT NO. (If appropriate, the applicable number under which the document was written.)

10a. DRDC PUBLICATION NUMBER (The official document number by which the document is identified by the originating activity. This number must be unique to this document.)	10b. OTHER DOCUMENT NO(s). (Any other numbers which may be assigned this document either by the originator or by the sponsor.)
DRDC-RDDC-2018-P059	

11a. FUTURE DISTRIBUTION WITHIN CANADA (Approval for further dissemination of the document. Security classification must also be considered.)

Public release

11b. FUTURE DISTRIBUTION OUTSIDE CANADA (Approval for further dissemination of the document. Security classification must also be considered.)

12. KEYWORDS, DESCRIPTORS or IDENTIFIERS (Use semi-colon as a delimiter.)

Lidar; Particle sizing; Clouds; Backscattering; Multiple scattering; Scattering, polarization

13. ABSTRACT/RÉSUMÉ (When available in the document, the French version of the abstract must be included here.)

The backscattering lidar depolarization parameter D of water droplets contains information on their size that can be directly modelled as a function of the forward scattering diffraction peak. Using a polarimetric Monte Carlo simulator, water clouds having different extinctions and droplet size distributions are analyzed to estimate their depolarization parameter at various backscattering off-axis angles. It is shown that depolarization parameter of the polarimetric phase function can be found using off-axis lidar measurements at multiple angles, and that it could be used to estimate the water cloud droplets size.